

# Retrofocusing techniques for high rate acoustic communications<sup>a)</sup>

Milica Stojanovic<sup>b)</sup>

Massachusetts Institute of Technology, Cambridge, Massachusetts 02139

(Received 8 June 2004; revised 14 December 2004; accepted 16 December 2004)

High rate underwater communications have traditionally relied on equalization methods to overcome the intersymbol interference (ISI) caused by multipath propagation. An alternative technique has emerged in the form of time-reversal, which comes at virtually no cost in computational complexity, but sacrifices the data rate and relies on the use of large arrays to reduce ISI. In this paper, spatiotemporal processing for *optimal* multipath suppression is addressed analytically. A communication link between a single element and an array is considered in several scenarios: uplink and downlink transmission, with and without channel state information and varying implementation complexity. Transmit/receive techniques are designed which simultaneously maximize the data detection signal-to-noise ratio and minimize the residual ISI, while maintaining maximal data rate in a given bandwidth and satisfying a constraint on transmitted energy. The performance of so-obtained focusing techniques is compared to the standard ones on a shallow water channel operating in a 5 kHz bandwidth around a 15 kHz center frequency. Results demonstrate benefits of focusing techniques whose performance is not conditioned on the array size. Optimal configurations are intended as a basis for adaptive system implementation in which channel estimates will replace the actual values. © 2005 Acoustical Society of America.

[DOI: 10.1121/1.1856411]

PACS numbers: 43.60.Ac, 43.60.Dh, 43.60.Fg, 43.60.Gk [EJS]

Pages: 1173–1185

## I. INTRODUCTION

High rate, bandwidth-efficient underwater communications have traditionally relied on adaptive equalization methods to overcome the intersymbol interference (ISI) caused by multipath propagation. Excellent performance of these receivers comes at a price of high computational complexity. While processing complexity can be somewhat reduced by use of sophisticated spatiotemporal multichannel equalizers,<sup>1</sup> retrofocusing techniques appear to offer a different approach. In traditional equalization, all of the signal processing is performed at the receiver side, while the transmitter uses standard signaling waveforms, which are designed *a priori*, and hence, are not matched to the channel. A different, and possibly better approach results if signal processing can be split between the transmitter and receiver. Such an approach forms the basis of spatiotemporal retrofocusing.

In its simplest form, retrofocusing is achieved by transmitting a time-reversed (or equivalently, phase-conjugated in the frequency domain) replica of a probe signal received earlier from the source location. This technique has been used for medical imaging, therapy, and material testing,<sup>2</sup> while more recently, time-reversal has been investigated as a communication technique that offers lower computational complexity as compared to traditional equalization.<sup>3–23</sup> However, in high rate communications time-reversal alone does not eliminate ISI, the fact that motivates present analysis and the search for optimal retrofocusing techniques.

## A. Previous work

Several research groups have been involved in application of time-reversal arrays to undersea acoustic communications, addressing active phase-conjugation for two-way communication, as well as passive phase-conjugation for one-way communication from a single-element source to an array.

The Scripps group has been engaged in experimental work, using large arrays to demonstrate spatial and temporal focusing of phase-coherent communication signals.<sup>3–8</sup> Communication begins with a single-element source transmitting the initial probe to an array. The array then uses the time-reversed replicas of the received, channel-distorted probe to generate *transmit* filters that are subsequently used for pulse-shaping the information sequence that is sent back to the source. This method of two-way communication is called active phase-conjugation. In one of the experiments, a 30 element array, operating at a center frequency of 3.5 kHz, was used to transmit PSK signals pulse-shaped at the transmitter array by a time-reversed replica of the probe signal received earlier. No signal processing was employed at the receiver, and transmission at 1 kbit/s over 10 km was reported.

The University of Washington group has addressed experimentally the technique of passive phase-conjugation,<sup>9–13</sup> in which the same principle of time-reversal is used for one-way communication. In this technique, the single-element source sends a probe, waits for the channel reverberation to subside, and then transmits the information-bearing signal to the array. The received channel-distorted probe is time-reversed and used at each array element as a *receive* filter for subsequent detection of the information-bearing signal. Peri-

<sup>a)</sup>Portion of this work was presented at the High Frequency Ocean Acoustics Conference, March 2004.

<sup>b)</sup>Electronic mail: millitsa@mit.edu

odic insertion of the probe signal is necessary to account for the time-variability of the channel. The technique was demonstrated experimentally using a 14 element array, operating in the 5–20 kHz band, to transmit data over distances of about 1 km. Transmission at 2 kbits/s was reported; however, such transmission could only be sustained for a short period of time, after which the probe signal had to be retransmitted to account for the channel time-variability (probe retransmission effectively reduced the data rate by a factor of 2). To recover the loss in data rate, decision-directed phase-conjugation was used, in which the detected data stream was used to regenerate the channel estimates. Passive phase conjugation was compared to standard equalization, showing that significant performance degradation, which increases with signal-to-noise ratio (SNR) and eventually leads to saturation, is the price to be paid for low computational complexity.<sup>14</sup>

In parallel with these experimental efforts that emphasize low-complexity processing using time-reversal, a third group of researchers at IST, Portugal, focused on analytical work.<sup>15–20</sup> Realizing that probe retransmission considerably reduces the effective data rate in both active and passive phase-conjugation, this group proposed the use of adaptive channel estimation to generate the up-to-date time-reversed filters directly from the received information-bearing signal, thus eliminating the need for probe retransmission (inevitably at the expense of increased computational complexity). This group also proposed the use of low-complexity adaptive equalization *in conjunction* with time-reversal.

As the early experiments devoted to implementing time-reversal in the ocean and testing the basic concepts have shown, suppression of multipath effects through time-reversal can be achieved at the expense of reduced data throughput and/or the need for a large array. For a better utilization of channel resources, additional signal processing is necessary to eliminate ISI and enable high-rate communications.

Ensuring ISI-free transmission in a system that has multiple transmit/receive elements is a major asset in a channel whose bandwidth is severely limited. In particular, it lays ground for capacity improvement through the use of space-time coding and multi-input multi-output (MIMO) signaling. This technique, developed originally for radio channels, was shown to increase the fundamental channel capacity in proportion to the number of transmit/receive elements used.<sup>24</sup> However, capacity-approaching codes are known only for ISI-free channels. MIMO signal processing for controlling the intersymbol and the inter-channel interference in underwater acoustic systems was addressed in the framework of multiple-user communications,<sup>25</sup> and, more recently, for single-user communications using multiple transmit elements.<sup>26</sup> Recent experimental results demonstrate large bandwidth efficiency improvement over acoustic channels, provided that accurate channel estimation is available and that residual ISI is kept at a minimum.

## B. Problem definition

While recent research demonstrates the potential of time-reversal in spatial localization of acoustical energy, it

often fails to recognize that time-reversal alone does not provide temporal focusing necessary to eliminate ISI caused by multipath propagation. Time-reversal recombines multipath energy in a manner of matched filtering, whose function is to maximize the SNR at a given time instant, and not to eliminate ISI. In fact, matched filtering *increases* temporal dispersion of the signal, i.e., the duration of the overall impulse response of the system. While SNR maximization is an appropriate optimization criterion for single pulse focusing, its application to communication problems, where a *sequence* of data-modulated pulses is transmitted at a high rate, must be approached judiciously. For signals that contain temporal dispersion, matched filter represents only the front end of the optimal receiver, and must be followed by a sequence estimator or an equalizer.<sup>27</sup>

Multipath components that remain after matched filtering contribute to residual ISI, whose severity depends on the channel. If not equalized, residual ISI may completely prevent detection. Increasing the number of array elements in a time-reversal array only helps to *reduce* residual ISI, but it does not eliminate it. Hence, if time-reversal is to be used toward eliminating the multipath distortion without sacrificing the data rate, it must be combined with equalization to remove residual ISI. However, the advantage of this approach to standard equalization that uses fixed transmitter wave forms is not apparent. The use of retrofocusing for *complete* suppression of multipath thus remains an open question.

In this paper, a solution is proposed to the following problem: If the channel responses between a single element and an array are known, determine the optimal transmit/receive technique that the two can use to simultaneously (i) eliminate ISI *and* (ii) maximize SNR, while maintaining *maximal* data rate in a given bandwidth and satisfying a constraint on transmitted energy. Note that because it allows for transmitter as well as receiver optimization, the solution differs from standard equalization. Also, because it explicitly requires minimization of ISI, it differs from time-reversal. The resulting system does *not* depend on the number of array elements to minimize the multipath distortion, i.e., it does not trade the computational complexity for the array size, but instead provides an answer for a variety of applications that cannot afford large arrays.

For those applications that also cannot afford processing power at both ends of the link, a constrained optimization problem is considered. A complexity restriction, likely to be imposed on the remote, single-element end, forces its transmit/receive filters to use no knowledge of the channel. The resulting one-sided focusing solution sacrifices some of the performance of the two-sided focusing in exchange for minimal implementation complexity. Analytical results are provided to quantify this trade-off.

A related question that emerges during the study of optimal focusing is the following: If the requirement for no ISI is relaxed, and the use of both channel-dependent transmit filtering *and* equalization at the receiver is allowed, what is the optimal system configuration, and how does its performance compare to that of optimal focusing? Analytical solution to this problem provides an upper bound on the perfor-

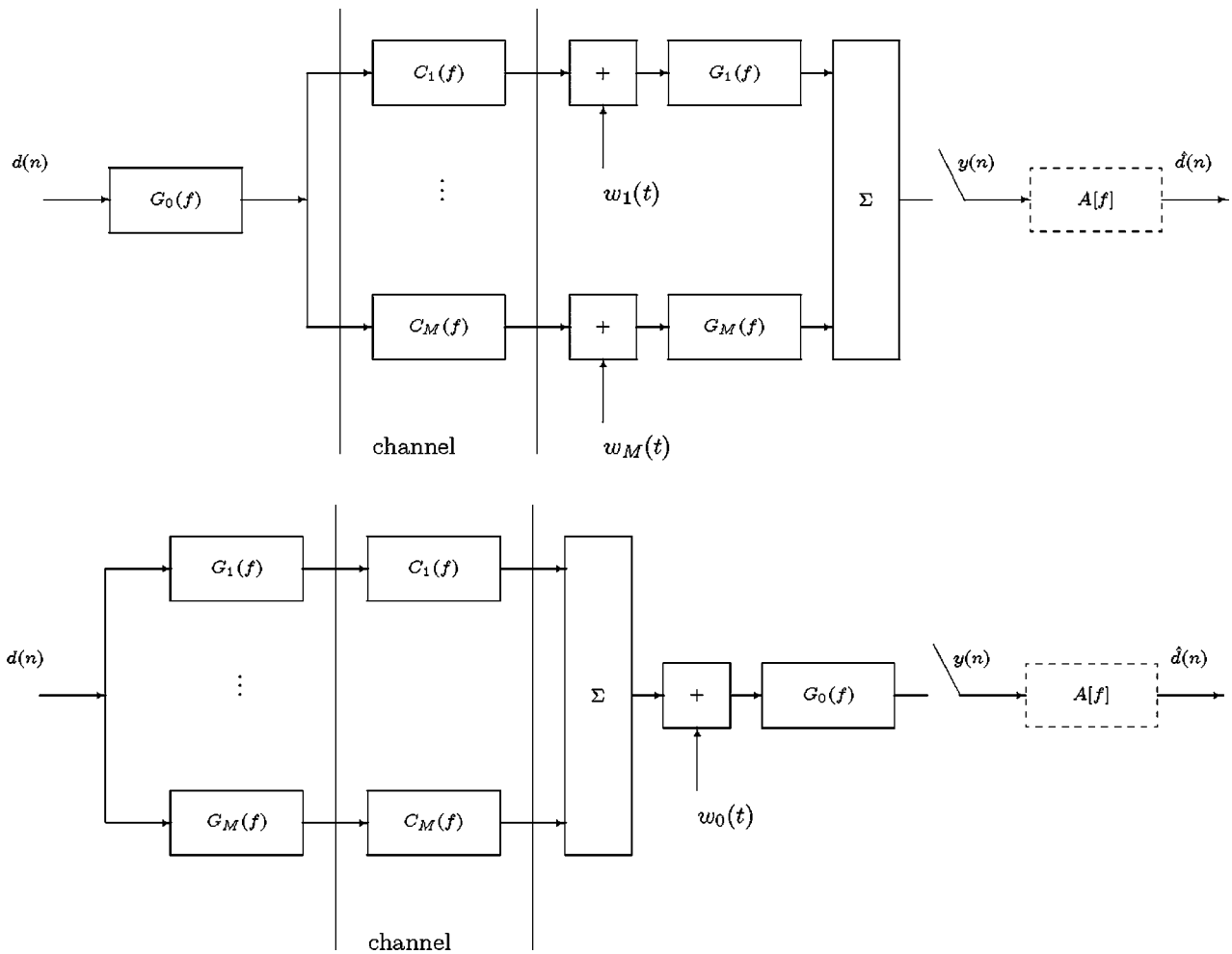


FIG. 1. Uplink (above) and downlink (below) transmission. An equalizer (dashed box) may or may not be used.

mance of all spatiotemporal processing methods.

System optimization is addressed in Sec. II. under various optimization criteria. In Sec. III., the performance of resulting techniques is compared through numerical computation of the analytical expressions for predicted performance of a system operating at 10 kbits/s over a 3 km shallow water channel. Results demonstrate the benefits of optimal focusing which outperforms time-reversal, and whose performance is not contingent on the array size. The conclusions are summarized in Sec. IV.

Optimal configurations discussed in this paper are intended as a basis for adaptive system implementation in which channel estimates will replace the unknown, time-varying responses. An adaptive channel estimation procedure, which uses a low-complexity decision-directed approach,<sup>28</sup> is suitable for this task.

## II. SYSTEM OPTIMIZATION

In this section, system optimization is addressed for uplink and downlink communication (to/from array), as shown in Fig. 1. Performance is assessed using SNR as the figure of merit, and compared to that of time-reversal, standard linear equalization, and transmit time-reversal in conjunction with equalization (receive time-reversal is identical to matched filtering, which, when followed by an equalizer, reduces to

standard equalization). System optimization is first addressed under no ISI requirement, while optimization of transmit filtering for use in conjunction with equalization is addressed subsequently.

### A. Transmitter/receiver optimization for no ISI (focusing)

The sequence of data symbols  $d(n)$  is transmitted at a symbol rate  $1/T$ . Referring to Fig. 1, the problem is to find the transmit/receive filters  $G_0(f)$  and  $G_1(f), \dots, G_M(f)$  such that the SNR at the receiver is maximized, subject to the constraint that there is no ISI in the decision variables  $\hat{d}(n) = y(nT)$ , and that finite transmitted energy per symbol  $E$  is used. The channel responses  $C_m(f)$ ,  $m = 1, \dots, M$ , and the power spectral density  $S_w(f)$  of the uncorrelated noise processes  $w_m(t)$ ,  $m = 0, \dots, M$ , are assumed to be known.

Let the composite equivalent baseband channel transfer function be denoted by

$$F(f) = G_0(f) \sum_{m=1}^M G_m(f) C_m(f). \quad (1)$$

The received signal after filtering is then given by

$$y(t) = \sum_n d(n) f(t - nT) + z(t) \quad (2)$$

where the noise  $z(t)$  has power spectral density

$$S_z(f) = S_w(f) \times \begin{cases} \sum_{m=1}^M |G_m^2(f)| & \text{for uplink transmission} \\ |G_0^2(f)| & \text{for downlink transmission.} \end{cases} \quad (3)$$

The requirement for no ISI is expressed as

$$F(f) = X(f), \quad (4)$$

where  $X(f)$  is a Nyquist transfer function, i.e., it is band-limited to  $|f| < 1/T$ , and its waveform in time,  $x(t)$ , satisfies the condition

$$x(nT) = \begin{cases} x_0 & \text{for } n=0 \\ 0 & \text{otherwise.} \end{cases} \quad (5)$$

Without the loss of generality, we take that  $X(f) = |X(f)|$ . For example,  $X(f)$  can be chosen as a raised cosine spectrum,<sup>27</sup> whose bandwidth  $B$  is controlled by the roll-off factor  $\alpha \in [0, 1]$ ,  $B = (1/T)(1 + \alpha)$ . When  $\alpha \rightarrow 0$ ,  $X(f) \rightarrow T$  for  $|f| \leq 1/2T$ , and no excess bandwidth is used, i.e., maximal symbol rate is achieved for which ISI-free transmission is possible within the available bandwidth.

When there is no ISI, the received signal, sampled at times  $nT$ , is given by

$$y(nT) = d(n)x_0 + z(nT) \quad (6)$$

and the SNR is

$$\text{SNR} = \frac{\sigma_d^2 x_0^2}{\sigma_z^2}. \quad (7)$$

where  $\sigma_d^2 = E\{|d^2(n)|\}$  and  $\sigma_z^2 = \int_{-\infty}^{+\infty} S_z(f) df$ .

The total transmitted energy is the energy of the signal  $u_0(t) = \sum_n d(n)g_0(t - nT)$  for the uplink scenario, or the sum of energies of the signals  $u_m(t) = \sum_n d(n)g_m(t - nT)$ ,  $m = 1, \dots, M$  for the downlink scenario. The power spectral density of these signals is  $S_{u_m}(f) = (1/T)S_d(f)|G_m(f)|^2$ , where  $S_d(f)$  is the power spectrum of the data sequence.<sup>27</sup> If the transmitted energy per symbol is set to  $E$ , assuming uncorrelated data symbols ( $S_d(f) = \sigma_d^2$ ), the energy constraint is expressed as

$$E = \sigma_d^2 \times \begin{cases} \int_{-\infty}^{+\infty} |G_0^2(f)| df, & \text{for uplink transmission} \\ \sum_{m=1}^M \int_{-\infty}^{+\infty} |G_m^2(f)| df, & \text{for downlink transmission.} \end{cases} \quad (8)$$

### 1. Unrestricted optimization (two-sided filter adjustment)

Let us first consider uplink transmission. Taking into account the energy constraint, and the no-ISI requirement,  $G_0(f) = X(f)/\sum_{m=1}^M G_m(f)C_m(f)$ , the SNR is expressed as

$$\begin{aligned} \text{SNR} &= \frac{Ex_0^2}{\sigma_z^2 \int_{-\infty}^{+\infty} |G_0^2(f)| df} \\ &= \frac{Ex_0^2}{\int_{-\infty}^{+\infty} \frac{X^2(f)}{|\sum_{m=1}^M G_m(f)C_m(f)|^2} df \int_{-\infty}^{+\infty} S_w(f) \sum_{m=1}^M |G_m^2(f)| df}. \end{aligned} \quad (9)$$

This function is to be maximized with respect to the receive filters  $G_m(f)$ ,  $m = 1, \dots, M$ . To do so, we use a two-step procedure, each step involving one Schwarz inequality. The first inequality states that

$$\left| \sum_{m=1}^M G_m(f)C_m(f) \right|^2 \leq \sum_{m=1}^M |G_m^2(f)| \sum_{m=1}^M |C_m^2(f)|, \quad (10)$$

where the equality holds for

$$G_m(f) = \alpha(f)C_m^*(f). \quad (11)$$

We note similarly with time-reversal in that receive filters should be proportional to the phase-conjugate of the channel transfer functions. However, there is room for additional improvement through optimization of the function  $\alpha(f)$ .

Denoting the composite channel power spectral density by

$$\gamma(f) = \sum_{m=1}^M |C_m^2(f)| \quad (12)$$

and using the inequality (10) we have that

SNR

$$\leq \frac{Ex_0^2}{\int_{-\infty}^{+\infty} \frac{X^2(f)}{\gamma(f) \sum_{m=1}^M |G_m^2(f)|} df \int_{-\infty}^{+\infty} S_w(f) \sum_{m=1}^M |G_m^2(f)| df} \quad (13)$$

Applying a second Schwarz inequality to the denominator of the SNR bound yields

$$\begin{aligned} &\int_{-\infty}^{+\infty} \frac{X^2(f)}{\gamma(f) \sum_{m=1}^M |G_m^2(f)|} df \int_{-\infty}^{+\infty} S_w(f) \sum_{m=1}^M |G_m^2(f)| df \\ &\geq \left[ \int_{-\infty}^{+\infty} \frac{X(f)}{\sqrt{\gamma(f)}} \sqrt{S_w(f)} df \right]^2, \end{aligned} \quad (14)$$

where the equality holds for

$$\frac{X(f)}{\sqrt{\gamma(f)S_w(f)}} = \beta \sum_{m=1}^M |G_m^2(f)| \quad (15)$$

and  $\beta$  is a constant. Combining the conditions (11) and (15) we obtain the optimal value

$$\alpha(f) = \frac{1}{\sqrt{\beta}} \frac{1}{S_w^{1/4}(f)} \frac{\sqrt{X(f)}}{\gamma^{3/4}(f)}. \quad (16)$$

The transmit filter is now obtained from the no-ISI condition (4) as

$$G_0(f) = \frac{X(f)}{\alpha(f)\gamma(f)} \quad (17)$$

and the constant  $\beta$  then follows from the energy constraint (8, uplink):

$$E = \sigma_d^2 \beta \int_{-\infty}^{+\infty} \sqrt{S_w(f)} \frac{X(f)}{\sqrt{\gamma(f)}} df. \quad (18)$$

The desired filters are given in the following:

$$G_0(f) = K(f) \sqrt{X(f)} \gamma^{-1/4}(f),$$

$$G_m(f) = K^{-1}(f) \sqrt{X(f)} \gamma^{-3/4}(f) C_m^*(f), \quad m = 1, \dots, M$$

where

$$K(f) = \sqrt{\frac{E/\sigma_d^2}{\int_{-\infty}^{+\infty} \sqrt{S_w(f)} \frac{X(f)}{\sqrt{\gamma(f)}} df}} S_w^{1/4}(f). \quad (19)$$

We can verify that the result reduces to the known case by setting  $M = 1$ .<sup>27</sup>

This selection of filters achieves maximal SNR,

$$\text{SNR}_2 = E x_0^2 \left[ \int_{-\infty}^{+\infty} \sqrt{S_w(f)} \frac{X(f)}{\sqrt{\gamma(f)}} df \right]^{-2}, \quad (20)$$

where the index “2” signifies the fact that both sides of the link adjust their filters in accordance with the channel.

Filter optimization in the downlink transmission case is accomplished similarly, by a double application of the Schwarz inequality. The resulting filters are given in the same form as for the uplink case, except that the factor  $K(f)$  is reciprocal of that given in Eq. (19). The same maximal SNR,  $\text{SNR}_2$  (20), is achieved.

## 2. Restricted optimization (one-sided filter adjustment)

We now turn to the situation in which one side of the communication link is restricted to have minimal complexity, such as when limited processing power is available at one end of the link. Namely, we constrain the single-element side to use a filter  $G_0(f)$  that is fixed, i.e., it may not be computed as a function of the channel responses.

To illustrate the optimization procedure, we look at the downlink transmission case. The no-ISI condition still must hold,  $F(f) = X(f)$ , and to maximize the SNR, this transfer function should be divided between the transmitter and receiver so that

$$G_0(f) = \beta \frac{\sqrt{X(f)}}{\sqrt{S_w(f)}}, \quad (21)$$

where  $\beta$  is a constant. For this selection, the SNR achieves the Schwarz inequality (matched filter) bound,

$$\text{SNR} = \frac{\sigma_d^2 \left| \int_{-\infty}^{+\infty} G_0(f) \sum_{m=1}^M G_m(f) C_m(f) df \right|^2}{\int_{-\infty}^{+\infty} S_w(f) |G_0(f)|^2 df}$$

$$\leq \sigma_d^2 \int_{-\infty}^{+\infty} \frac{1}{S_w(f)} \left| \sum_{m=1}^M G_m(f) C_m(f) \right|^2 df. \quad (22)$$

Applying the Schwarz inequality (10) to the above integrand yields

$$\text{SNR} \leq \sigma_d^2 \int_{-\infty}^{+\infty} \frac{1}{S_w(f)} \gamma(f) \sum_{m=1}^M |G_m^2| df \quad (23)$$

with equality holding for  $G_m(f) = \alpha(f) C_m^*(f)$ ,  $m = 1, \dots, M$ . Combining this condition with the matched-filter requirement (21) and the no-ISI constraint, we obtain the optimal value

$$\alpha(f) = \frac{1}{\beta} \frac{\sqrt{X(f)}}{\gamma(f)} \sqrt{S_w(f)}. \quad (24)$$

The constant  $\beta$  can now be determined from the energy constraint (8, downlink):

$$E = \sigma_d^2 \frac{1}{\beta^2} \int_{-\infty}^{+\infty} S_w(f) \frac{X(f)}{\gamma(f)} df. \quad (25)$$

The desired filters are given in the following:

$$G_0(f) = K^{-1}(f) \sqrt{X(f)},$$

$$G_m(f) = K(f) \sqrt{X(f)} \gamma^{-1}(f) C_m^*(f), \quad m = 1, \dots, M$$

where

$$K(f) = \sqrt{\frac{E/\sigma_d^2}{\int_{-\infty}^{+\infty} S_w(f) \frac{X(f)}{\gamma(f)} df}} S_w^{1/2}(f). \quad (26)$$

This selection of filters achieves the maximal SNR available with one-sided adjustment,

$$\text{SNR}_1 = E x_0 \left[ \int_{-\infty}^{+\infty} S_w(f) \frac{X(f)}{\gamma(f)} df \right]^{-1}. \quad (27)$$

In the uplink transmission case with restricted computational complexity, the transmit filter is simply chosen as the standard (e.g., square-root raised cosine) function, and an analogous optimization procedure results in the following solution:

$$G_0(f) = K \sqrt{X(f)},$$

$$G_m(f) = K^{-1} \sqrt{X(f)} \gamma^{-1}(f) C_m^*(f), \quad m = 1, \dots, M$$

where

$$K = \sqrt{\frac{E/\sigma_d^2}{x_0}}. \quad (28)$$

The same SNR,  $\text{SNR}_1$  (27), is achieved.

Comparing the SNR available with and without complexity restriction, we find that  $\text{SNR}_1 \leq \text{SNR}_2$ . The two SNRs are equal only when  $\gamma(f)$  is proportional to  $S_w(f)$ .

In what follows, we shall focus on the usual case of white noise,  $S_w(f) = N_0$ . Note that the factors  $K(f)$  then become constants independent of frequency in both two-sided and one-sided focusing, and the same set of filters may be used for uplink and downlink transmission. The SNR expressions reduce to

$$\text{SNR}_2 = \frac{E}{N_0} x_0^2 \left[ \int_{-\infty}^{+\infty} \frac{X(f)}{\sqrt{\gamma(f)}} df \right]^{-2} \quad (29)$$

and

$$\text{SNR}_1 = \frac{E}{N_0} x_0 \left[ \int_{-\infty}^{+\infty} \frac{X(f)}{\gamma(f)} df \right]^{-1}. \quad (30)$$

We now want to compare these values of SNR, achieved through optimal focusing, to the SNR achieved by time-reversal and methods based on equalization.

## B. Time-reversal performance with residual ISI

When no care is taken to ensure focusing, the samples of the received signal contain residual ISI:

$$y(nT) = f(0)d(n) + \sum_{k \neq n} f(kT)d(n-k) + z(nT). \quad (31)$$

Assuming uncorrelated data symbols, the SNR is given by

$$\text{SNR}_0 = \frac{\sigma_d^2 |f^2(0)|}{\sigma_d^2 \sum_{k \neq 0} |f^2(kT)| + \sigma_z^2}. \quad (32)$$

We look at the following scenarios. On the uplink, the transmitter uses a standard filter,  $G_0(f) = K_u \sqrt{X(f)}$ , and the receiver uses  $G_m(f) = G_0^*(f) C_m^*(f)$ ,  $m = 1, \dots, M$ . This scenario is analogous to ideal (noiseless) passive phase-conjugation. On the downlink, the transmitter uses  $G_m(f) = K_d \sqrt{X(f)} C_m^*(f)$ ,  $m = 1, \dots, M$ , and the receive filter is simply  $G_0(f) = \sqrt{X(f)}$ . This scenario is analogous to active phase-conjugation. The constants  $K_u$ ,  $K_d$  are determined from the energy constraint (8). The resulting SNR is the same in the uplink and the downlink scenarios, and it is given by

$$\text{SNR}_0 = \frac{\frac{E}{N_0}}{\frac{E}{N_0} \rho + \frac{x_0}{\int_{-\infty}^{+\infty} X(f) \gamma(f) df}}, \quad (33)$$

where

$$\rho = \frac{\sum_{k \neq 0} |f^2(kT)|}{|f^2(0)|} = \frac{T \int_{-1/2T}^{+1/2T} X \gamma[f]^2 df}{\left| \int_{-\infty}^{+\infty} X(f) \gamma(f) df \right|^2} - 1 \quad (34)$$

and  $X \gamma[f]$  is used to denote the folded spectrum of  $X(f) \gamma(f)$ :

$$X \gamma[f] = \frac{1}{T} \sum_{k=-\infty}^{+\infty} X\left(f + \frac{k}{T}\right) \gamma\left(f + \frac{k}{T}\right). \quad (35)$$

It is interesting to observe that as the noise vanishes, i.e.,  $E/N_0 \rightarrow +\infty$ , unlike with optimal focusing when  $\text{SNR}_{1,2} \rightarrow +\infty$ , the performance of time-reversal saturates:  $\text{SNR}_0 \rightarrow 1/\rho$ . The value of  $\rho$  depends on the channel characteristics, expressed through the function  $\gamma(f)$ , and the system bandwidth, expressed through the function  $X(f)$ .

## C. Time-reversal performance with equalization

The performance of time-reversal saturates because of residual ISI. To overcome this limitation, an equalizer may be used. We look at the downlink scenario, where an optimal, minimum mean squared error (MMSE) linear processor is employed. It consists of a receiving matched filter followed by a symbol rate sampler and a linear MMSE equalizer. For the received signal samples given in the form (31) with uncorrelated data sequence, the MMSE equalizer has a transfer function

$$A[f] = \frac{\sigma_d^2 F^*[f]}{\sigma_d^2 |F[f]|^2 + S_z[f]}, \quad (36)$$

where  $F[f]$  is the folded spectrum of the overall response  $F(f)$ , and  $S_z[f]$  is the power spectral density of the discrete-time noise process  $z(nT)$ . The receiving filter is matched to the overall response,

$$G_0(f) = \sum_{m=1}^M G_m^*(f) C_m^*(f) \quad (37)$$

so that  $F(f) = |G_0^2(f)|$ , and, hence,  $S_z[f] = N_0 F[f]$ . The equalizer transfer function thus reduces to

$$A[f] = \frac{\frac{\sigma_d^2}{N_0}}{1 + \frac{\sigma_d^2}{N_0} F[f]}. \quad (38)$$

The SNR at the equalizer output is<sup>27</sup>

$$\text{SNR} = \frac{1}{\text{MSE}} - 1 = \left[ T \int_{-1/2T}^{+1/2T} \frac{1}{1 + \frac{\sigma_d^2}{N_0} F[f]} df \right]^{-1} - 1. \quad (39)$$

For the transmit filter selection as in active phase-conjugation,  $G_m(f) = K_d \sqrt{X(f)} C_m^*(f)$ ,  $m = 1, \dots, M$ , we have that

$$\frac{\sigma_d^2}{N_0} F(f) = \frac{E/N_0}{\int_{-\infty}^{+\infty} X(f) \gamma(f) df} X(f) \gamma^2(f). \quad (40)$$

This transfer function is used to compute the resulting SNR (39):

$$\text{SNR}_{3,\text{tr}} = \left[ T \int_{-1/2T}^{+1/2T} \frac{1}{1 + \frac{E/N_0}{\int_{-\infty}^{+\infty} X(f) \gamma(f) df} X \gamma^2[f]} df \right]^{-1} - 1 \quad (41)$$

where  $X \gamma^2[f]$  is the folded spectrum of  $X(f) \gamma^2(f)$ .

In the uplink transmission case, time-reversal filtering at the receiver is followed by equalization. Because passive phase-conjugation is equivalent to matched filtering, and the transmitter uses a fixed filter, this case is identical to standard equalization, which is treated next.

## D. Equalizer performance

A standard equalizer does not rely on time-reversal at the transmitter, but instead uses pre-determined, channel-independent filters. In the downlink case, the transmit filters are  $G_m(f) = K_d \sqrt{X(f)}$ ,  $m = 1, \dots, M$ , and we have that

$$\frac{\sigma_d^2}{N_0} F(f) = \frac{E/N_0}{M x_0} X(f) \Sigma^2(f), \quad (42)$$

where

$$\Sigma(f) = \left| \sum_{m=1}^M C_m(f) \right|. \quad (43)$$

Note that this case may represent a poor system design as transmission over multiple channels with different delays creates additional time spreading, and the channel transfer functions add directly in the above expression, possibly in a destructive manner. The resulting SNR is computed from Eq. (39):

$$\text{SNR}_{3,\text{down}} = \left[ T \int_{-1/2T}^{+1/2T} \frac{1}{1 + \frac{E/N_0}{M \int_{-\infty}^{+\infty} X(f) df} X \Sigma^2[f]} df \right]^{-1} - 1, \quad (44)$$

where  $X \Sigma^2[f]$  is the folded spectrum of  $X(f) \Sigma^2(f)$ .

In the uplink scenario, the MMSE linear processor consists of a bank of matched filters,  $G_m(f) = G_0^*(f) C_m^*(f)$ ,  $m = 1, \dots, M$ , as in passive phase-conjugation, whose outputs are summed, sampled at the symbol rate, and processed by a linear equalizer. This process is also called multichannel equalization. The MMSE equalizer is again defined by Eq. (38) where the overall transfer function is now  $F(f) = |G_0^2(f)| \gamma(f)$ . For the standard transmit filter selection,  $G_0(f) = K_u \sqrt{X(f)}$ , we have that

$$\frac{\sigma_d^2}{N_0} F(f) = \frac{E/N_0}{x_0} X(f) \gamma(f). \quad (45)$$

The resulting SNR is computed from Eq. (39):

$$\text{SNR}_{3,\text{up}} = \left[ T \int_{-1/2T}^{+1/2T} \frac{1}{1 + \frac{E/N_0}{\int_{-\infty}^{+\infty} X(f) df} X \gamma[f]} df \right]^{-1} - 1, \quad (46)$$

where, as before,  $X \gamma[f]$  is the folded spectrum of  $X(f) \gamma(f)$ .

Comparing uplink and downlink equalization, we have that  $\text{SNR}_{3,\text{up}} \geq \text{SNR}_{3,\text{down}}$ . The two are equal if the channel transfer functions  $C_m(f)$ ,  $m = 1, \dots, M$  are identical and constant within the signal bandwidth. It is not clear, however, how  $\text{SNR}_{3,\text{down}}$  compares with  $\text{SNR}_{3,\text{tr}}$ , i.e., what is the advantage, if any, of using transmit time-reversal in conjunction with equalization. This question gives rise to a broader one of optimal transmit filtering for use with equalization.

## E. Transmitter/receiver optimization for a system with equalization

So far, we have looked at optimal focusing (filter optimization under no-ISI constraint) and at MMSE equalization using *a priori* selected transmit filters. However, it is possible to look at a system in which both channel-dependent transmit filtering *and* equalization are used. In other words, if the requirement for no ISI is relaxed in the optimal system design, and the equalizer is allowed at the receiver, the question is what transmit/receive filtering should be used to maximize the SNR. Note that because this optimization criterion is less restrictive than that of focusing (the no-ISI constraint has been removed) improved performance may be expected. Also, performance must be improved with respect to standard equalization, which represents only a special case of transmit filter selection.

For any given transmit filtering, an optimal linear receiver consists of a matched filter (or a bank of matched filters for the uplink scenario) followed by a symbol-spaced MMSE equalizer (36). Both the matched filter and the equalizer transfer functions depend on the transmit filter selection, and consequently, so does the achieved SNR. We want to find the transmit filter(s) for which the SNR at the equalizer output (39) is maximized. Transmit filtering, in turn, will determine receive filtering and the equalizer.

Let us first consider the uplink case. Maximizing the SNR is equivalent to minimizing the MSE, which is defined by the overall transfer function  $F(f) = |G_0^2(f)| \gamma(f)$ . We assume that the system operates in minimal bandwidth  $B$  required to support ISI-free transmission at symbol rate  $1/T$ , i.e.,  $G_0(f)$  is zero for  $|f| > 1/2T$ . Then, the optimization problem is to find the function  $G_0(f)$  for which

$$\text{MSE}_{\text{up}} = T \int_{-1/2T}^{+1/2T} \frac{1}{1 + \frac{\sigma_d^2}{N_0 T} |G_0^2(f)| \gamma(f)} df \quad (47)$$

is minimized, subject to the constraint on transmitted energy,

$$\sigma_d^2 \int_{-1/2T}^{1/2T} |G_0^2(f)| df = E. \quad (48)$$

In the downlink case, the MSE is defined by the overall transfer function  $F(f) = |\sum_{m=1}^M G_m(f) C_m(f)|^2$ , and we want to find a set of functions  $G_m(f)$ ,  $m = 1, \dots, M$  for which

$$\text{MSE}_{\text{down}} = T \int_{-1/2T}^{+1/2T} \frac{1}{1 + \frac{\sigma_d^2}{N_0 T} |\sum_{m=1}^M G_m(f) C_m(f)|^2} df \quad (49)$$

is minimized, subject to the constraint on transmitted energy,

$$\sigma_d^2 \int_{-1/2T}^{1/2T} \sum_{m=1}^M |G_m^2(f)| df = E. \quad (50)$$

Realizing that the downlink MSE is bounded by

$$\text{MSE}_{\text{down}} \geq T \int_{-1/2T}^{+1/2T} \frac{1}{1 + \frac{\sigma_d^2}{N_0 T} |\alpha^2(f)| \gamma(f)} df, \quad (51)$$

which is achieved for  $G_m(f) = \alpha(f)C_m^*(f)$ ,  $m = 1, \dots, M$ , the downlink optimization problem can be reduced to the same form as that of the uplink problem. Namely, if we define

$$\Phi(f) = \frac{\sigma_d^2}{N_0 T} \times \begin{cases} |G_0(f)|^2 & \text{for uplink transmission} \\ |\alpha(f)|^2 \gamma(f) & \text{for downlink transmission,} \end{cases}$$

$$|f| \leq \frac{1}{2T} \quad (52)$$

then

$$\text{MSE} = T \int_{-1/2T}^{1/2T} \frac{1}{1 + \Phi(f) \gamma(f)} df \quad (53)$$

is to be minimized with respect to a real, non-negative function  $\Phi(f)$ , subject to the constraint that

$$T \int_{-1/2T}^{1/2T} \Phi(f) df = \frac{E}{N_0}. \quad (54)$$

Using the Lagrange method, we form

$$\Lambda(\Phi) = T \int_{-1/2T}^{1/2T} \frac{1}{1 + \Phi(f) \gamma(f)} df + \lambda \left[ T \int_{-1/2T}^{1/2T} \Phi(f) df - \frac{E}{N_0} \right], \quad (55)$$

where  $\lambda$  is a constant. Differentiating the above function with respect to  $\Phi$ , and setting the derivative equal to zero, provides the following solution:

$$\Phi(f) = \frac{1}{\gamma(f)} \left[ \frac{1}{\sqrt{\lambda}} \sqrt{\gamma(f)} - 1 \right], \quad f \in B_0 = \left[ -\frac{1}{2T}, \frac{1}{2T} \right]. \quad (56)$$

Substituting this solution into the constraint (54) we obtain

$$\frac{1}{\sqrt{\lambda}} = K_0 = \frac{\frac{E}{N_0} + T \int_{-1/2T}^{1/2T} \frac{1}{\gamma(f)} df}{T \int_{-1/2T}^{1/2T} \frac{1}{\sqrt{\gamma(f)}} df}. \quad (57)$$

To ensure a valid solution for  $\Phi(f)$ , we must verify that  $K_0 \geq 1/\sqrt{\gamma_{\min}}$ ,  $\forall f \in [-1/2T, 1/2T]$ . This condition will hold if  $K_0 \geq 1/\sqrt{\gamma_{\min}}$ , where  $\gamma_{\min}$  is the smallest value of  $\gamma(f)$  within the available bandwidth,

$$\gamma_{\min} = \min_{f \in B_0} \{\gamma(f)\}. \quad (58)$$

If this is not the case, the expression (56) does not represent a valid solution. We then modify the solution as follows:

$$\Phi(f) = \begin{cases} \frac{1}{\gamma(f)} [K_L \sqrt{\gamma(f)} - 1] & f \in B_L \subset B_0 \\ 0 & \text{otherwise} \end{cases}, \quad (59)$$

where  $K_L$  is determined from the energy constraint (54),

$$K_L = \frac{\frac{E}{N_0} + T \int_{B_L} \frac{1}{\gamma(f)} df}{T \int_{B_L} \frac{1}{\sqrt{\gamma(f)}} df} \quad (60)$$

and  $B_L$  is the maximal bandwidth for which  $K_L \geq 1/\sqrt{\gamma(f)}$ ,  $\forall f \in B_L$ .

To gain insight into this definition, we note that whenever it is decided a priori that  $\Phi(f)$  is zero for some frequency region  $\bar{B}_L$  (the complement of  $B_L$  within  $B_0$ ), the MSE (53) can be expressed as

$$\text{MSE} = T \int_{\bar{B}_L} df + T \int_{B_L} \frac{1}{1 + \Phi(f) \gamma(f)} df \quad (61)$$

and the energy constraint becomes

$$T \int_{B_L} \Phi(f) df = \frac{E}{N_0}. \quad (62)$$

The solution (59) then represents  $\Phi(f)$  for which the second MSE term is minimized subject to the energy constraint. In order to minimize the first MSE term as well, the smallest possible frequency region  $\bar{B}_L$  (i.e., the largest  $B_L$ ) should be chosen, hence the definition of  $B_L$ .

We further define the set of frequencies  $B_L$  to be

$$B_L = \{f \in B_0 : \gamma(f) \geq \gamma_L\}, \quad (63)$$

where  $\gamma_L$  is the smallest value of  $\gamma(f)$  within  $B_0$ , for which  $K_L \geq 1/\sqrt{\gamma_L}$ ,

$$\gamma_L = \min_{f \in B_0 : K_L \geq 1/\sqrt{\gamma_L}} \{\gamma(f)\}. \quad (64)$$

When  $B_L$  is defined via the threshold  $\gamma_L$ , then this threshold should be minimized. Separation of the frequency regions  $B_L$  and  $\bar{B}_L$  based on thresholding of the channel function  $\gamma(f)$  is intuitively satisfying, because it states that if transmit energy is limited, it should not be wasted on those regions where  $\gamma(f)$  is low.

The solution for  $K_L$  can be obtained numerically, starting with  $B_L = B_0 = [-1/2T, 1/2T]$ . If the resulting  $K_L = K_0 \geq 1/\sqrt{\gamma_{\min}}$ , then  $\Phi(f)$  has a full nonzero solution (56). If this is not the case,  $K_L$  is computed from Eq. (60) iteratively, increasing  $\gamma_L$  from the initial value  $\gamma_{\min}$  by a small amount  $\Delta \gamma_L$  in each step, until the condition  $K_L \geq 1/\sqrt{\gamma_L}$  is met. The search for  $\gamma_L$  then stops, and the solution for  $\Phi(f)$  follows from Eq. (59).

The desired transmit/receive filters are given in the following:

$$\text{uplink: } G_0(f) = K \sqrt{\Phi(f)},$$

$$G_m(f) = K \sqrt{\Phi(f)} C_m^*(f), \quad m = 1, \dots, M,$$

$$\text{downlink: } G_m(f) = K \sqrt{\Phi(f)} \gamma^{-1/2}(f) C_m^*(f),$$

$$m = 1, \dots, M,$$

$$G_0(f) = K \sqrt{\Phi(f)} \gamma^{1/2}(f),$$

where

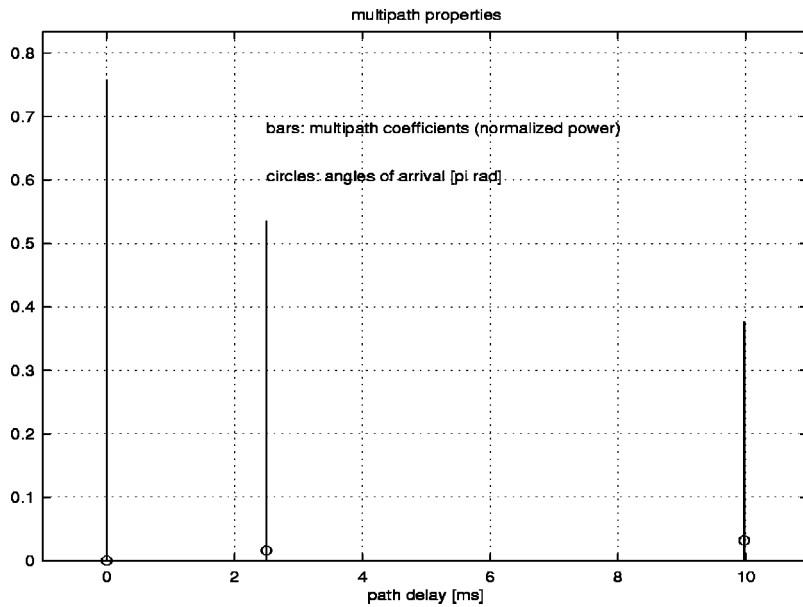


FIG. 2. Multipath characteristics of the example channel: path gain magnitudes  $|c_p|$  and angles of arrival  $\theta_p$  are shown at corresponding delays  $\tau_p$  (reference delay is  $\tau_0=0$ ).

$$K = \sqrt{N_0 T / \sigma_d^2}. \quad (65)$$

The equalizer transfer function (up to the normalizing constant  $\sigma_d^2/N_0$ ) is the same for uplink and for downlink transmission:

$$A[f] = \frac{1}{1 + \Phi(f)\gamma(f)}, \quad |f| \leq \frac{1}{2T}. \quad (66)$$

This system achieves the SNR,

$$\text{SNR}_4 = \left\{ 1 - T \int_{B_L} df + \left[ T \int_{B_L} \frac{1}{\sqrt{\gamma(f)}} df \right]^2 \times \left[ \frac{E}{N_0} + T \int_{B_L} \frac{1}{\gamma(f)} df \right]^{-1} \right\}^{-1} - 1. \quad (67)$$

In the case when  $B_L = B_0$ , it is easily shown that

$$\text{SNR}_4 = \text{SNR}_2 + \frac{\text{SNR}_2}{\text{SNR}_1} - 1 \geq \text{SNR}_2. \quad (68)$$

Thus, this signaling scheme outperforms optimal focusing. The question, of course, is how great is the difference in performance.

### III. PERFORMANCE COMPARISON

In this section, we use an illustrative example to compare the performance of various techniques discussed: optimal focusing with two-sided filter adjustment, optimal focusing with one-sided filter adjustment, time-reversal, time-reversal in conjunction with equalization, standard equalization (with fixed transmit filters), and equalization using optimized transmit filters. Performance is evaluated through numerical computation of the analytical SNR expressions for a particular channel model.

#### A. Channel model

The channel model is based on geometry of shallow water multipath. We look at repeated surface-bottom reflections and take into account a certain number of multipath

arrivals,  $P$ . Each multipath component is characterized by a gain  $c_p$ , delay  $\tau_p$ , and angle of arrival  $\theta_p$ , which are computed from the propagation path length  $l_p$ . The path gain magnitude is computed as  $|c_p| = \Gamma_p / \sqrt{A(l_p)}$ , where  $\Gamma_p \leq 1$  may be used to model loss due to reflection (we choose each reflection to introduce a  $\sqrt{2}$  loss in amplitude) and  $A(l_p)$  is the nominal acoustic propagation loss,  $A(l_p) = l_p^k [a(f_c)]^{l_p}$ , calculated assuming practical spreading,  $k = 1.5$ , a carrier frequency  $f_c = 15$  kHz, and absorption according to Thorp. [For  $f_c$  in kHz,  $a(f_c)$  is given in dB/km as  $10 \log a(f_c) = 0.11 f_c^2 / (1 + f_c^2) + 44 f_c^2 / (4100 + f_c^2) + 2.75 \times 10^{-4} f_c^2 + 0.003$ .] The path gain phase is computed as  $\angle c_p = -2\pi f_c \tau_p$ . Observed across the array, there is a phase delay  $\varphi_p = 2\pi(d/\lambda_c)\sin\theta_p$  between the elements spaced by  $d$ , where  $\lambda_c = c/f_c$ , and  $c = 1500$  m/s is the nominal sound speed. In reference to the first element, the channel transfer functions are given by

$$C_m(f) = \sum_{p=0}^{P-1} c_{m,p} e^{-j2\pi f \tau_p},$$

where

$$c_{m,p} = c_p e^{-j(m-1)\varphi_p}, \quad m = 1, \dots, M. \quad (69)$$

As an example, we use a channel of depth 75 m, range of 3 km, and the system mounted near the bottom. Three propagation paths are taken into account (direct, surface reflected, and surface-bottom-surface reflected). Figure 2 shows the resulting multipath profile of the channel. We note that the total multipath spread is 10 ms, which is on the order of that observed experimentally.

The channel function  $\gamma(f)$  is shown in Fig. 3 for  $M = 4$  and  $M = 32$ . Shown on the same plot is the desired system response  $X(f)$  chosen as a raised cosine with roll-off factor close to 0, which provides maximal bit rate for ISI-free transmission in a bandwidth  $B = 1/T$ . The symbol duration is chosen to be  $T = 0.2$  ms, corresponding to the bandwidth of 5 kHz and transmission at 10 kbits/s if 4-PSK is used, or 15 kbits/s if 8-PSK is used. The impulse response of

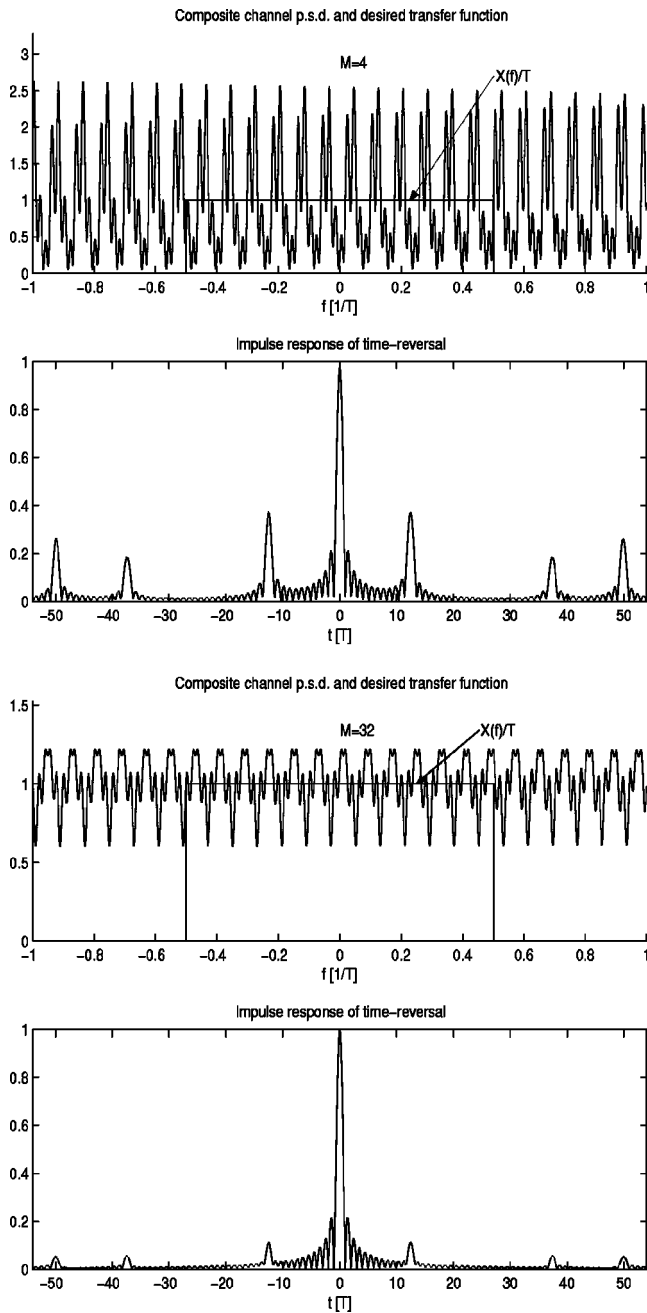


FIG. 3. Composite channel power spectral density  $\gamma(f)$ , and the impulse response of time-reversal which corresponds to  $X(f)\gamma(f)$ . Multipath coefficients are normalized such that  $M\sum_p |c_p^2| = 1$ , and half-wavelength spacing between array elements is used.

the overall system obtained with time-reversal is also shown, and it is evidently far from ideal. As the number of array elements is increased,  $\gamma(f)$  tends to flatten out, resulting in better, but not complete suppression of multipath through time-reversal.

## B. Performance analysis

Figure 4 summarizes performance results for the two examples. Let us focus on the  $M=4$  case. We first confirm that two-sided focusing [Eq. (29), solid curve labeled “ $\Delta$ ”] outperforms one-sided focusing [Eq. (30), dashed curve labeled “ $\Delta$ ”], but more interestingly, we observe that the difference in performance is small. This is an encouraging ob-

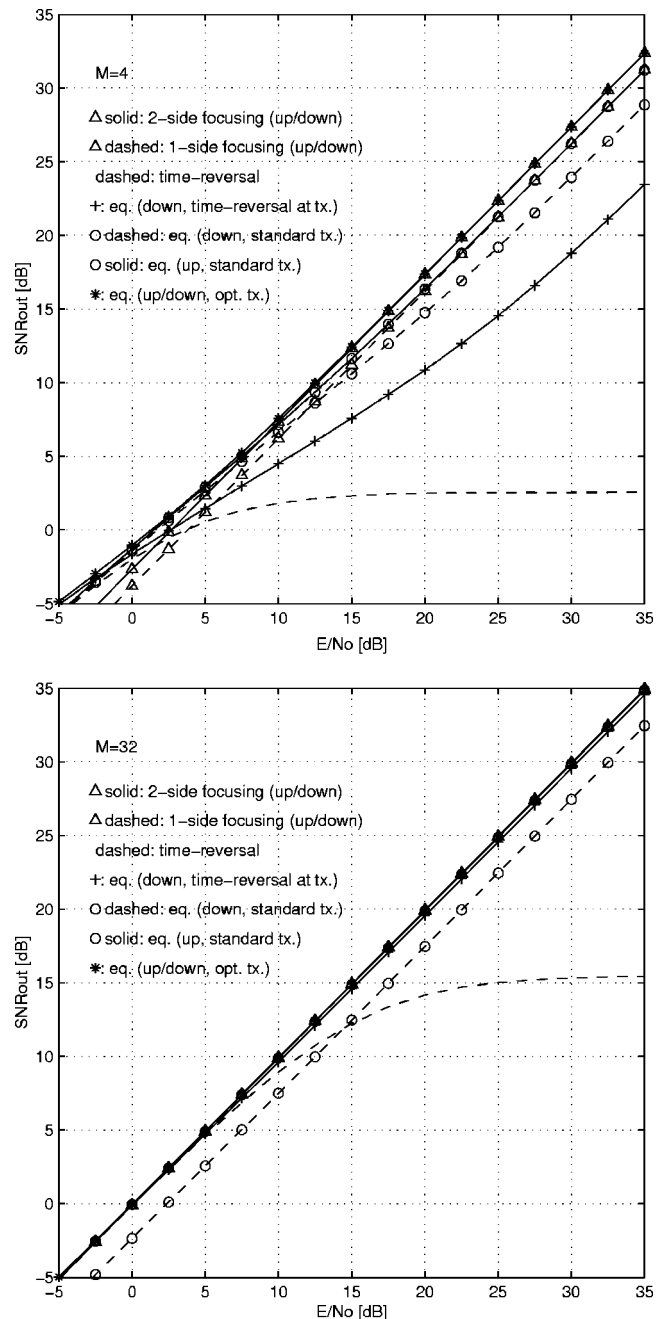


FIG. 4. Performance of various techniques on the example channel: output SNR vs  $E/N_0$  for fixed number of array elements  $M$ .

servation from the viewpoint of designing a practical system with restricted processing complexity. The performance of time-reversal [Eq. (33), dashed curve] is inferior to optimal focusing and to all other schemes at practical values of SNR. By practical, those values are meant that yield at least several dB of output SNR, as this is required for an adaptive system to perform in a decision-directed manner. The loss of time-reversal becomes quite large even at a moderate  $E/N_0$  of 10–15 dB, and the performance saturates thereafter at a value  $1/\rho$  determined by the channel (34). Some of the loss is recovered by the use of an equalizer in conjunction with transmit time-reversal [Eq. (41), curve labeled “+”]. However, it is interesting to observe that this system compares poorly with the standard equalizer that uses square-root raised cosine transmit filters and equal energy allocation

across the array [Eq. (44), dashed curve labeled “○”]. Standard downlink equalization is inferior to its uplink counterpart [Eq. (46), solid curve labeled “○”], which offers a consistently good performance. Note that this performance is closely matched by one-sided focusing at moderate to high SNR. Finally, we confirm that equalization using optimized transmit filters [Eq. (67), curve labeled “\*”] provides an upper bound on the performance of all other schemes. More important, we observe that this scheme offers negligible improvement over focusing, which allows a much easier implementation.

With  $M=32$ , the performance of time-reversal improves; however, the saturation effect is still notable. Nonetheless, it has to be noted that at low and moderate  $E/N_0$  up to about 10 or 15 dB, with the increased number of elements, time-reversal becomes the technique of choice as it offers near-optimal performance at minimal computational complexity. Equalization in conjunction with transmit time-reversal now outperforms standard downlink equalization, while the performance of both focusing methods, as well as that of standard uplink equalization, tends to the same optimal curve. Comparing the performance achieved with 32 and with 4 elements demonstrates that optimal focusing is much less sensitive to the array size than either of the techniques based on time-reversal (recall also that the power in the channel is kept constant with changing  $M$ ).

Performance sensitivity to the array size is summarized in Fig. 5, which shows the output SNR as a function of  $M$  for a given symbol SNR  $E/N_0$ . Two values of  $E/N_0$  are taken as an example, 10 and 20 dB. In each instance, we note superiority of focusing methods over time-reversal. Performance of focusing methods shows fast improvement with initial increase in  $M$ , and a small increment thereafter. Hence, good performance can be achieved without unduly increasing the number of array elements. For example, if one-sided focusing is used, and  $E/N_0 \geq 10$  dB, increasing the number of elements beyond 6 offers less than 3 dB total improvement in performance. In contrast to this situation, time-reversal steadily gains in performance within the range of  $M$  shown; however, it fails to achieve the performance of focusing methods. Most important, we observe that at moderate to high symbol SNR, one-sided focusing needs a relatively small number of array elements to approach the optimal performance.

Results of Fig. 5 also offer an interesting comparison between standard equalization and equalization in conjunction with transmit time-reversal. Using time-reversal at the transmitter offers an improvement provided that  $M$  is greater than a certain number. In the example considered, this number is 11 at  $E/N_0$  of 10 dB, and 8 at  $E/N_0$  of 20 dB.

So far, we have considered up to  $M=32$  elements, but it is interesting to observe the performance of time-reversal with a further increase in  $M$ , to see what array size is needed to bring its performance to that of other techniques. Figure 6 shows the performance of time-reversal for an extended range of  $M$ . Shown on the same plot is the performance of optimal focusing, which, on this scale, is indistinguishable from the system bound or multichannel equalization. An interesting effect is immediately apparent: the performance of

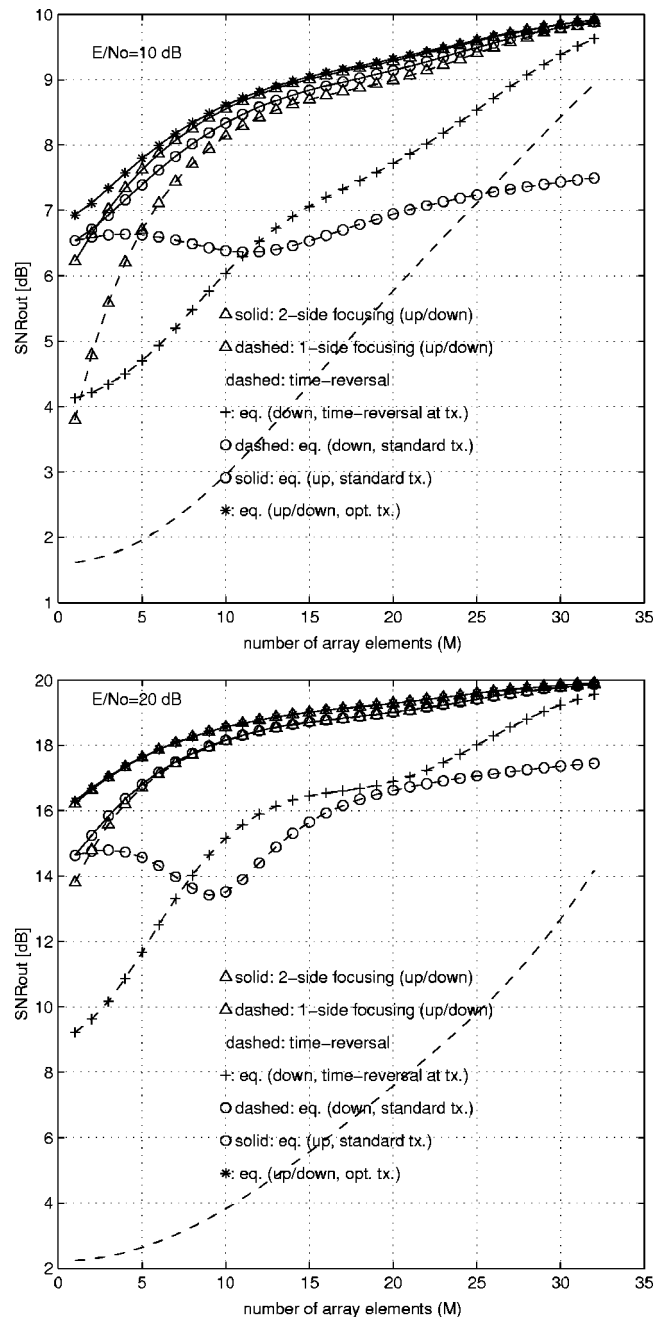


FIG. 5. Performance of various techniques on the example channel: output SNR vs  $M$  for fixed symbol SNR  $E/N_0$ .

time-reversal does not consistently improve with increasing  $M$  (as does the performance of focusing techniques and uplink equalization) but instead exhibits an oscillatory behavior, tending to the optimum only as  $M \rightarrow \infty$ . The values of  $M$  for which the performance is best are those values for which it happens so that the composite channel function  $\gamma(f)$  flattens out almost completely, i.e.,  $\gamma(f) \approx 1$ . At these values of  $M$ , time-reversal approaches the performance bound. However, due to the nature of the function  $\gamma(f)$ , the performance does not remain at optimum, but deviates from it with an increase in  $M$ . This fact underlines the suboptimality of system design based on time-reversal only. In practice, it could be difficult to rely on finding the optimal number of elements every time the array is deployed and system configuration changes.

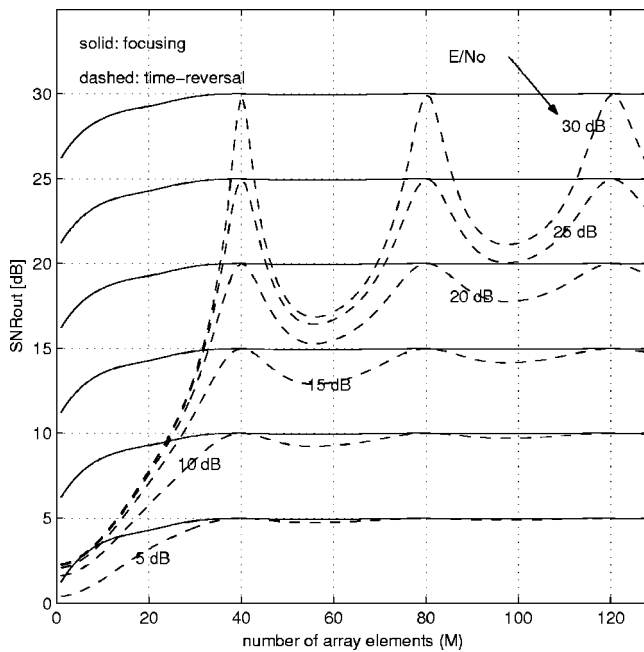


FIG. 6. Performance of time-reversal and optimal focusing for extended range of  $M$ .

Finally, we investigate performance sensitivity to the changes in multipath composition and the array element spacing, both of which influence the channel function  $\gamma(f)$ . Figure 7 shows performance results obtained for the same channel model, but with six, instead of three multipath components taken into account. The total multipath spread is now somewhat greater than 60 ms, with the additional arrivals' strength approximately 9, 12, and 15 dB below the principal arrival. The performance differs little as compared to the three-path channel. If anywhere, the difference can be seen when only a few elements are used—the performance of time-reversal is then worse on the six-path channel, while that of other techniques is better. More important, we ob-

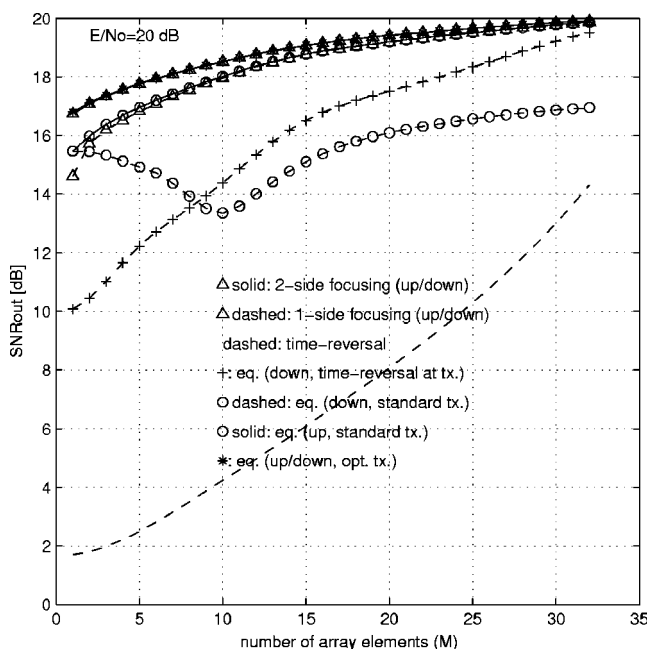


FIG. 7. Output SNR vs  $M$  for the six-path channel model,  $d = \lambda_c/2$ .

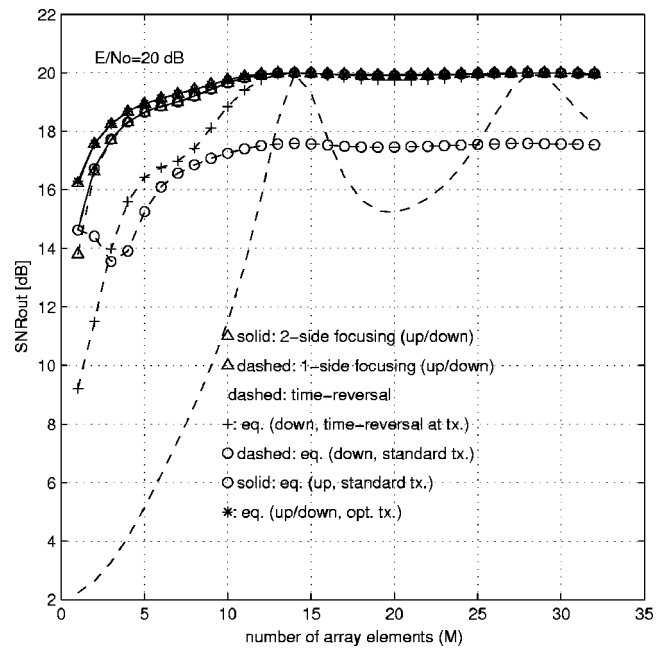


FIG. 8. Output SNR vs  $M$  for the three-path channel model,  $d = 1.41\lambda_c$ .

serve that the same conclusions regarding performance comparison between different techniques hold in the presence of extended multipath. To assess performance sensitivity to changes in relative strength of the multipath arrivals, a hypothetical case of a lossless six-path channel was investigated. Suffice it to say that the same general conclusions were made in this case.

The effect of changing the array element spacing is illustrated in Fig. 8. This figure shows performance results for the original three-path channel, but with  $d = 1.41\lambda_c$  instead of  $d = \lambda_c/2$ . Evidently, the performance of time-reversal shows more sensitivity to the changes in the array element spacing than the other techniques (the same would be true for changes in the carrier frequency). The optimum is now approached with a smaller number of elements (this number corresponds to the same total array length, i.e., 40 elements spaced by  $\lambda_c/2$  or 14 elements spaced by  $1.41\lambda_c$  in the example considered). However, the improvement in performance is not consistent with an increase in the element spacing. For a given number of elements  $M > 1$ , performance improves with an initial increase in element spacing, but exhibits an oscillatory behavior afterwards. For example, with  $M = 4$ , performance starts to degrade after element spacing increases beyond  $5\lambda_c$ . With elements spaced by  $10\lambda_c$ , at  $E/N_0 = 20$  dB, the output SNR does not exceed a value of about 8 dB if more than two elements are used in a time-reversal array. Compared to this situation, performance of retrofocusing techniques shows negligible sensitivity to the changes in element spacing.

#### IV. CONCLUSION

A number of techniques have been investigated for communication over an underwater acoustic link where one end is equipped with a single transmit/receive element and another with an array. To achieve maximal bit rate within a fixed bandwidth, an optimization criterion of maximizing the

data detection SNR, while eliminating or minimizing the residual ISI was chosen. Transmit/receive filters were obtained analytically for uplink and downlink transmission, with varying degrees of system complexity. The so-obtained optimal techniques were compared to standard time-reversal and equalization.

Because it ignores residual ISI, time-reversal exhibits performance saturation, and strongly depends on the use of a large array. When this can be afforded (e.g., in a network whose base station uses an array to isolate multiple users) time-reversal offers a solution for minimal-complexity processing. With a smaller array, however, standard equalization outperforms time-reversal, and the use of equalization in conjunction with transmit time-reversal does not guarantee performance improvement over standard equalization, unless the number of elements exceeds a certain value. The proposed method of spatiotemporal retrofocusing guarantees maximal SNR and elimination of ISI for an arbitrary array size. It outperforms time-reversal at the expense of additional filtering. The filters needed for optimal focusing include phase-conjugation augmented by a channel-dependent scaling function. If filter adjustment is constrained to the array side only, one-sided focusing offers an excellent trade-off between complexity and performance. Its performance has only a small loss with respect to the two-sided focusing, and it stays close to that of uplink multichannel equalization. It thus represents a solution for systems that cannot deploy large arrays and have limited processing power. In addition, when two-way communication is to be established over a white-noise channel, the same set of filters can be used for transmission and reception.

The system analysis was completed by optimizing both ends of an equalization based system. While it is unlikely that a practical system would be based on this approach due to the difficulty of finding optimal filters, it provides an upper bound on the performance of all other techniques. Results demonstrate that optimal focusing performs very close to this bound.

Future work will concentrate on an experimental validation of spatiotemporal focusing aided by adaptive channel estimation. Two types of errors will guide the system performance: the error due to noise and the error due to time-variability of the channel. In particular, the latter may prove as the limiting factor for the performance of an acoustic system with a long round-trip delay and high rate of channel variation. Future analytical work will address system optimization with imperfect channel knowledge.

- <sup>1</sup>M. Stojanovic, J. Catipovic, and J. Proakis, "Reduced-complexity multi-channel processing of underwater acoustic communication signals," *J. Acoust. Soc. Am.* **98**, 961–972 (1995).
- <sup>2</sup>M. Fink, F. Wu, J.-L. Tomas, and D. Cassereau, "Time-reversal of ultrasonic fields—Parts I, II and III," *IEEE Trans. Ultrason. Ferroelectr. Freq. Control* **39**, 555–592 (1992).
- <sup>3</sup>W. A. Kuperman, W. S. Hodgkiss, H. C. Song, T. Akal, C. Ferla, and D. R. Jackson, "Phase conjugation in the ocean: Experimental demonstration of an acoustic time-reversal mirror," *J. Acoust. Soc. Am.* **103**, 25–40 (1998).
- <sup>4</sup>W. S. Hodgkiss, H. C. Song, W. A. Kuperman, T. Akal, C. Ferla, and D. R. Jackson, "A long-range and variable focus phase-conjugation experiment in shallow water," *J. Acoust. Soc. Am.* **105**, 1597–1604 (1999).
- <sup>5</sup>W. S. Hodgkiss, J. D. Skinner, G. E. Edmonds, R. A. Harriss, and D. E.

- Ensberg, "A high frequency phase-conjugation array," in Proceedings of the IEEE Oceans'01 Conference, pp. 1581–1585, 2001.
- <sup>6</sup>J. S. Kim, H. C. Song, and W. A. Kuperman, "Adaptive time-reversal mirror," *J. Acoust. Soc. Am.* **109**, 1817–1825 (2001).
- <sup>7</sup>G. Edelmann, W. S. Hodgkiss, W. A. Kuperman, and H. C. Song, "Underwater acoustic communication using time-reversal," in Proceedings of the IEEE Oceans'01 Conference, 2001.
- <sup>8</sup>H. C. Song, G. Edelmann, S. Kim, W. S. Hodgkiss, W. A. Kuperman, and T. Akal, "Low and high frequency ocean acoustic phase conjugation experiments," *Proc. SPIE* **4123**, 104–108 (2000).
- <sup>9</sup>D. Jackson and D. Dowling, "Phase-conjugation in underwater acoustics," *J. Acoust. Soc. Am.* **89**, 171–181 (1991).
- <sup>10</sup>D. Rouseff, D. R. Jackson, W. L. J. Fox, C. D. Jones, J. A. Ritcey, and D. R. Dowling, "Underwater acoustic communication by passive-phase-conjugation: Theory and experimental results," *IEEE J. Ocean. Eng.* **26**, 821–831 (2001).
- <sup>11</sup>D. Jackson, J. A. Ritcey, W. L. J. Fox, C. D. Jones, D. Rouseff, and D. R. Dowling, "Experimental testing of passive phase-conjugation for underwater acoustic communication," in Proceedings of the 34th Asilomar Conference, 2000, pp. 680–683.
- <sup>12</sup>J. Flynn, W. L. J. Fox, J. A. Ritcey, D. R. Jackson, and D. Rouseff, "Decision-directed passive phase-conjugation for underwater acoustic communications with results from a shallow-water trial," in Proceedings of the 35th Asilomar Conference, 2001, pp. 1420–1427.
- <sup>13</sup>D. Rouseff, J. A. Flynn, W. L. J. Fox, and J. A. Ritcey, "Decision-directed passive phase-conjugation for underwater acoustic communication: experimental results," in Proceedings of the IEEE Oceans'02 Conference (2002).
- <sup>14</sup>J. A. Flynn, W. L. J. Fox, J. A. Ritcey, and D. Rouseff, "Performance of reduced-complexity multi-channel equalizers for underwater acoustic communications," in Proceedings of the 36th Asilomar Conference, 2002, Vol. 1, pp. 453–460.
- <sup>15</sup>J. Gomes and V. Barroso, "The performance of sparse time-reversal mirrors in the context of underwater communications," in Proceedings of the 10th IEEE Workshop on Statistical Signal and Array Processing, 2000, pp. 727–731.
- <sup>16</sup>J. Gomes and V. Barroso, "A matched-field processing approach to underwater acoustic communication," in Proceedings of the IEEE Oceans'99 Conference, 1999, pp. 991–995.
- <sup>17</sup>J. Gomes and V. Barroso, "Asymmetric underwater acoustic communication using time-reversal mirror," in Proceedings of the IEEE Oceans'01 Conference, 2000.
- <sup>18</sup>J. Gomes and V. Barroso, "Wavefront segmentation in phase conjugate arrays for spatially modulated acoustic communication," in Proceedings of the IEEE Oceans'01 Conference, 2001, pp. 2236–2243.
- <sup>19</sup>J. Gomes and V. Barroso, "Ray-based analysis of a time-reversal mirror for underwater acoustic communication," in Proceedings of the IC-ASSP'00 Conference, 2000, pp. 2981–2984.
- <sup>20</sup>J. Gomes and V. Barroso, "Time-reversed communication over Doppler-spread underwater channels," in Proceedings of the ICASSP'02 Conference, 2002, pp. 2849–2852(III).
- <sup>21</sup>P. Hursky, M. Porter, J. Rice, and V. McDonald, "Passive phase-conjugate signaling using pulse-position modulation," in Proceedings of the IEEE Oceans'01 Conference, 2001.
- <sup>22</sup>T. C. Yang, "Temporal resolutions of time-reversal and passive phase-conjugation for underwater acoustic communications," *IEEE J. Ocean. Eng.* **28**, 229–245 (2003).
- <sup>23</sup>J. Skim and K. C. Shin, "Multiple focusing with adaptive time-reversal mirror," *J. Acoust. Soc. Am.* **115**, 600–606 (2004).
- <sup>24</sup>D. Gesbert, M. Shafi, D. Shiu, P. J. Smith, and A. Naguib, "From theory to practice: An overview of MIMO space-time coded wireless systems," *IEEE J. Sel. Areas Commun.* **21**, 281–302 (2003).
- <sup>25</sup>M. Stojanovic and Z. Zvonar, "Multichannel processing of broadband multiuser communication signals in shallow water acoustic channels," *IEEE J. Ocean. Eng.* **21**, 156–166 (1996).
- <sup>26</sup>D. Kilfoyle, J. Preisig, and A. Baggeroer, "Spatial modulation over partially coherent multi-input/multi-output channels," *IEEE Trans. Signal Process.* **51**, 794–804 (2003).
- <sup>27</sup>J. G. Proakis, *Digital Communications* (Mc-Graw Hill, New York, 1995).
- <sup>28</sup>M. Stojanovic, "Efficient acoustic signal processing based on channel estimation for high rate underwater information," *J. Acoust. Soc. Am.* (submitted) (available at <http://www.mit.edu/millitsa/publications.html>)